

## Electronic Supplementary Information

### Fourier transform infrared spectroscopy imaging as a screening tool to predict the grade and invasiveness of urothelial carcinoma of the bladder

Monika Kujdowicz<sup>1,2</sup>, David Perez-Guaita<sup>3\*</sup>, Piotr Chlost<sup>4</sup>, Krzysztof Okon<sup>1</sup> and Kamilla Malek<sup>2\*</sup>

<sup>1</sup> Department of Pathomorphology, Faculty of Medicine, Jagiellonian University Medical College, Krakow, Grzegorzecka 16, 31-531, Poland

<sup>2</sup> Faculty of Chemistry, Jagiellonian University, Krakow, Gronostajowa 2, 30-387, Poland

<sup>3</sup> Department of Analytical Chemistry, University of Valencia, 50 Dr. Moliner Street, Research Building, 46100 Burjassot, Valencia, Spain

<sup>4</sup> Department of Urology, Medical Faculty, Jagiellonian University Medical College, Krakow, Jakubowskiego 2, 30-688, Poland

**Table S1.** Positions of FTIR bands with their assignment to vibrational modes and biomolecules.<sup>10,15,21,37</sup>

Band [cm <sup>-1</sup> ]	Assignment
<b>967</b>	DNA; v(CNC)
<b>995</b>	RNA, glycogen; carbohydrate rings stretch and deformation
<b>1026</b>	Glycogen; δ(COH)
<b>1052</b>	Sugar moieties in DNA, polysaccharides, glycoproteins, collagen; v(C–O)
<b>1081</b>	Collagen, nucleic acids, phosphate-containing molecules, glycogen; v <sub>s</sub> (PO <sub>2</sub> <sup>-</sup> ), v(CC)
<b>1119-1111</b>	Polysaccharides, RNA, lactate; v(C-O), v(CC-OC)
<b>1154</b>	Glycogen, v <sub>as</sub> (CO-O-C)
<b>1200</b>	Collagen, v(COH, COC)
<b>1233</b>	Nucleic acids and other phosphate-containing molecules, v <sub>as</sub> (PO <sub>2</sub> <sup>-</sup> ); collagens, amide III
<b>1280</b>	Collagens, amide III,
<b>1335</b>	Collagens amide III:
<b>1370-1393</b>	free fatty acids and amino acids; v <sub>s</sub> (COO <sup>-</sup> )
<b>1450</b>	Proteins, lipids, carbohydrates; δ(CH <sub>2</sub> , CH <sub>3</sub> )
<b>1516</b>	Tyrosine residue, elastin; v(CC) <sub>ring</sub>
<b>1544</b>	Proteins; amide II; δ(NH) + v(C-N)
<b>1573</b>	Lipids, proteins, nucleic acids; v(C=N, C=C)
<b>1591</b>	free amino acids; v <sub>as</sub> (COO <sup>-</sup> )
<b>1637</b>	Proteins (β-sheets); amide I; collagen and elastin: v(C=O) + δ(N-H)
<b>1652</b>	Proteins (α-helix); amide I; v(C=O) + δ(N-H)
<b>1673</b>	Amide I; v(C=O) + δ(N-H)
<b>1687</b>	Proteins (β-turns); amide I, DNA; v(C=O)+δ(N-H), v(C=C, C=O)
<b>1743</b>	Triglycerides, phospholipids; v(C=O) ester group

v – stretching mode, as – antisymmetric, s - symmetric; δ – in-plane deformation.

**Table S2.** The position of regression vectors for the constructed models for BC classification (in  $\text{cm}^{-1}$ ). Bold numbers indicate the specific IR features of the epithelium and subepithelium.

N (ve-) vs BC (ve+)		Tni (ve-) vs Tinv (ve+)		HG (ve-) vs LG (ve+) BC		N (ve-) vs BC (ve+)		Tni (ve-) vs Tinv (ve+)	
Epithelium						Subepithelium			
ve-	ve+	ve-	ve+	ve-	ve+	ve-	ve+	ve-	ve+
1697	1683	<b>1590</b>	<b>1660</b>	1660	1682	1697	1683	<b>1682</b>	<b>1652</b>
1670	<b>1608</b>	<b>1552</b>	<b>1565</b>	1633	1609	1672	<b>1657</b>	<b>1640</b>	<b>1623</b>
1586	<b>1547</b>	<b>1524</b>	1477	1576	1547	1585	<b>1635</b>	<b>1544</b>	1562
1397	<b>1485</b>	1460	<b>1431</b>	1487	1457	<b>1547</b>	<b>1558</b>	1464	1447
1310	<b>1447</b>	<b>1337</b>	<b>1165</b>	1435	1215	1398	1414	<b>1364</b>	<b>1397</b>
<b>1140</b>	1413	<b>1226</b>	<b>1158</b>	1164	1043	1311	<b>1247</b>	<b>1214</b>	<b>1136</b>
1043	<b>1060</b>	<b>1188</b>	<b>1108</b>	980	992	1049	996	<b>1082</b>	<b>1068</b>
	996	<b>1043</b>				<b>1010</b>		<b>1023</b>	<b>980</b>

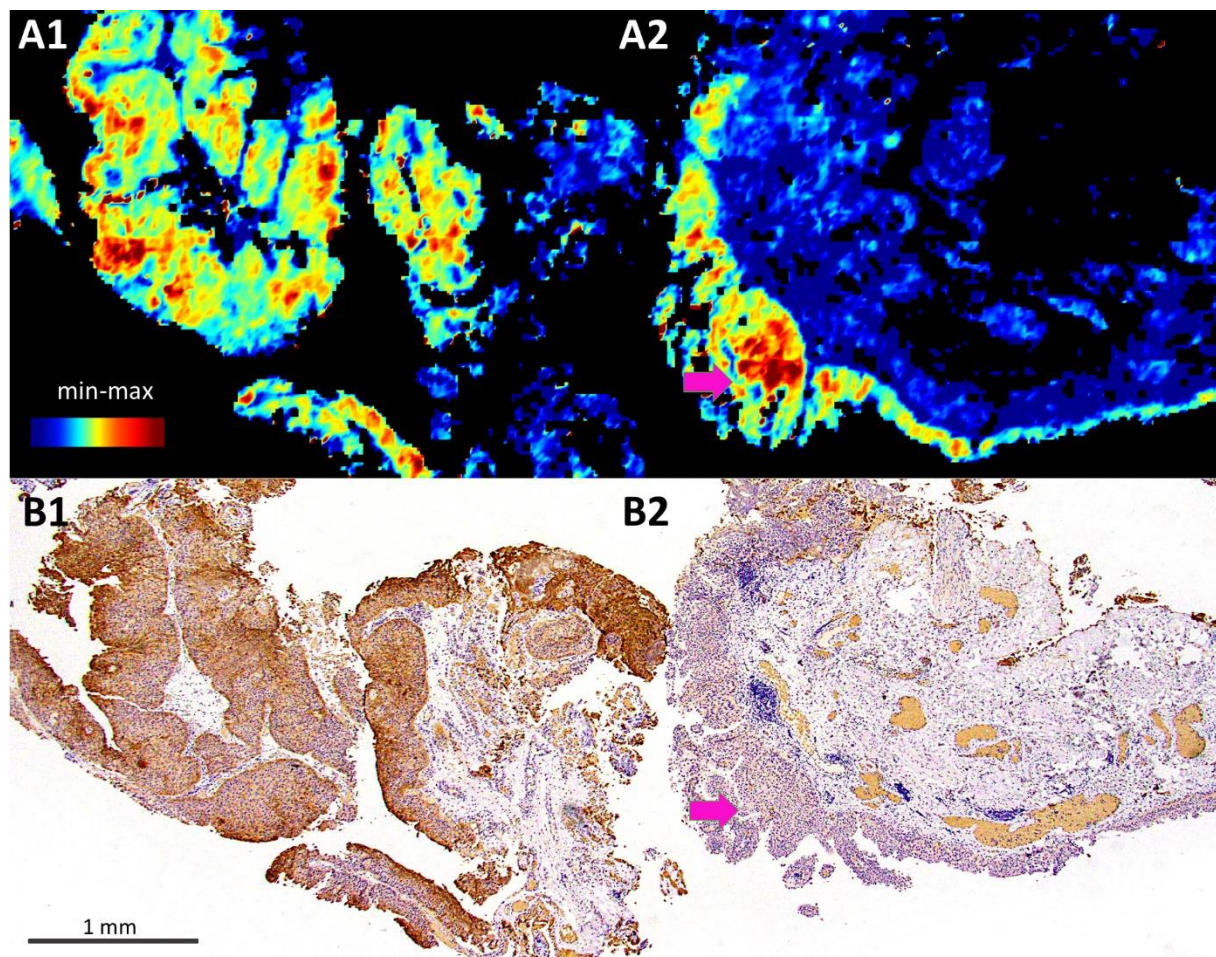


**Figure S1.** The comparison of IR distribution images for carbohydrates (**A1, A2**) and IHC Glut-1 expression (**B1, B2**, magnification 2 $\times$ ) for two excision samples from the T0 patient. Pink arrows in **A2** and **B2** indicate the early neoplastic changes which were not recognised in IHC.

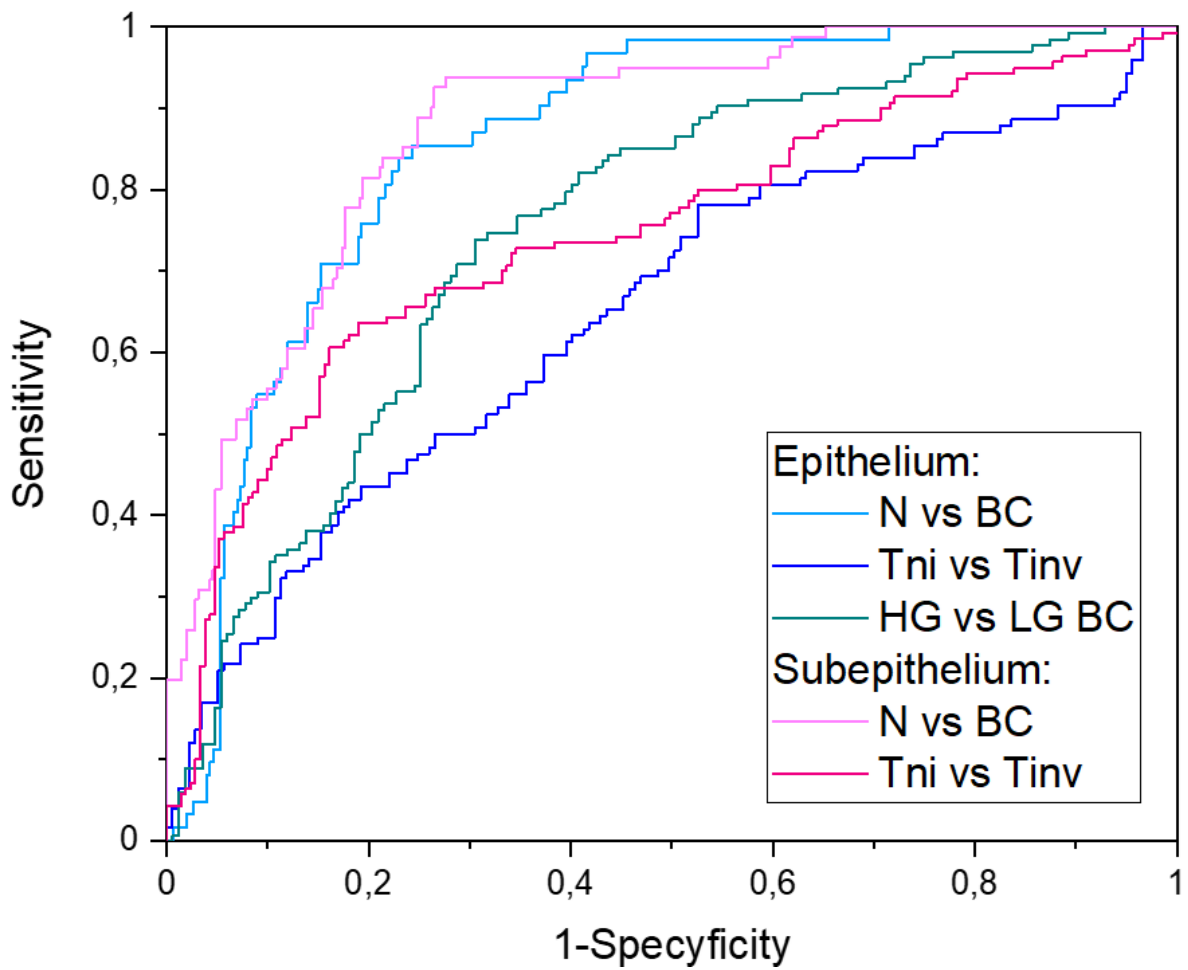


**Figure S2.** Area Under the Receiver Operation Curves for the cross validation of the patient groups.

Legend: Epithelium (n=417): n(N) = 62, n(Tni) = 124, n(Tinv) = 177, n(LG) = 167, n(HG) = 134; Subepithelium (n=494): n(N) = 81, n(Tni) = 140, n(Tinv) = 206.

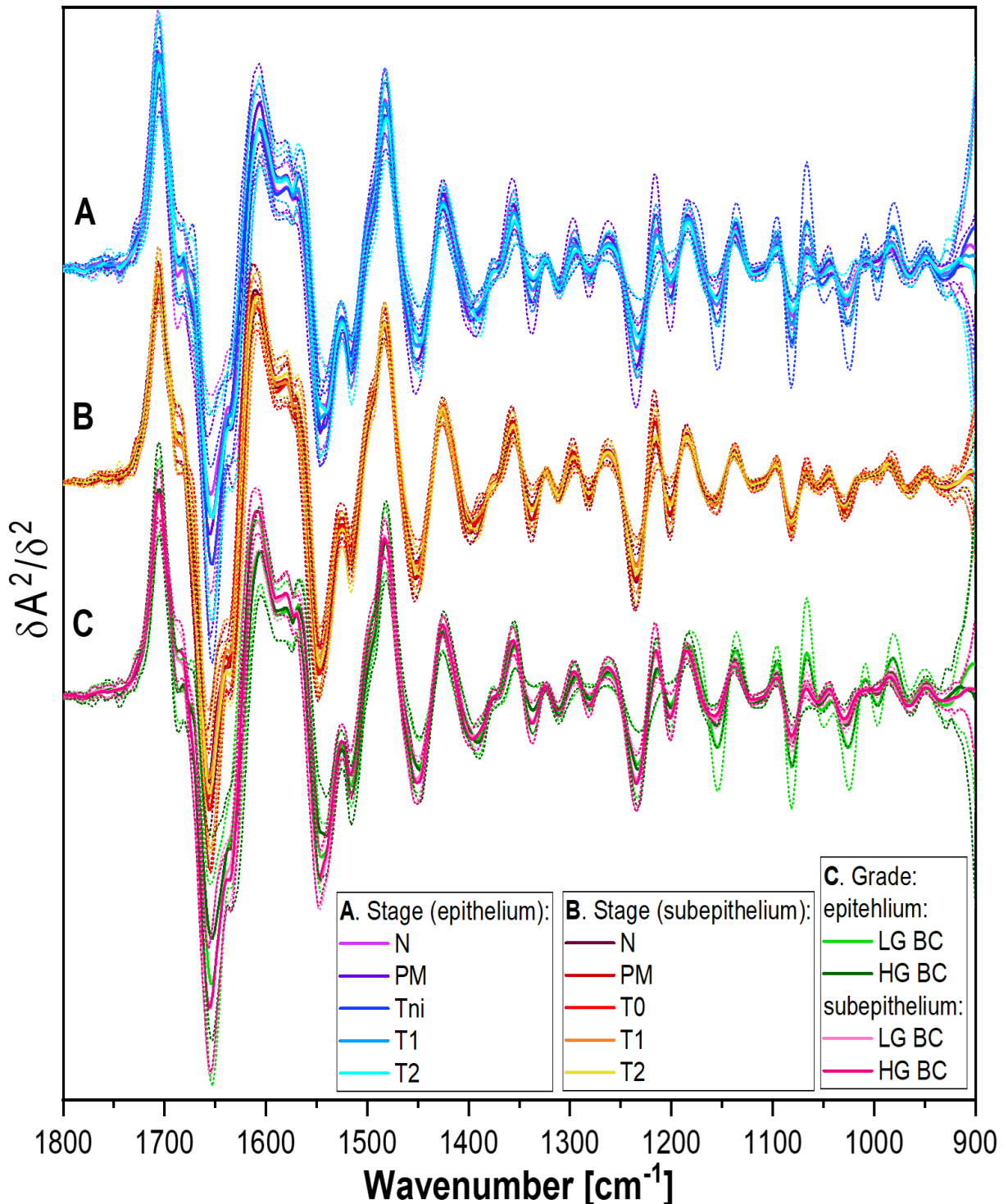


**Figure S3.** Averaged second derivatives IR spectra ( $\pm$ SD, marked with dotted lines) subjected to the epithelial and subepithelial bladder tissue (extracted from classes of UHCA).

Legend: Epithelium (n=417): n(N) = 62, n(PM) = 44, n(Tni) = 124, n(T1) = 94, n( $\geq$ T2) = 83, n(LG) = 167, n(HG) = 134; Subepithelium (n=494): n(N) = 81, n(PM) = 61, n(Tni) = 140, n(T1) = 122, n( $\geq$ T2) = 84; and Tinv is T1 +  $\geq$ T2.

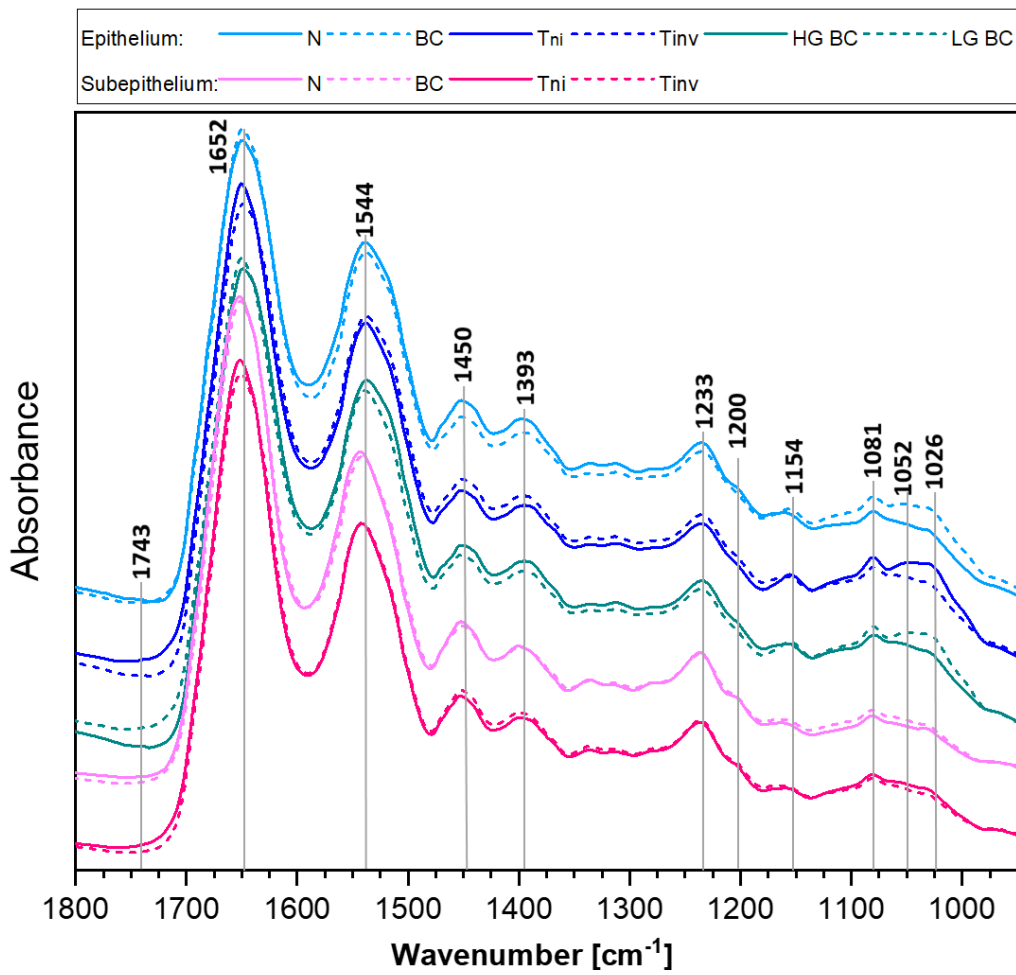


**Figure S4.** Averaged absorbance FTIR spectra of the epithelial and subepithelial tissues of the bladder (extracted from classes of UHCA).

Legend: Epithelium (n=417): n(N) = 62, n(Tni) = 124, n(Tinv) = 177, n(LG) = 167, n(HG) = 134; Subepithelium (n=494): n(N) = 81, n(Tni) = 140, n(Tinv) = 206.